

# Potential energy surface prediction of Alumina polymorphs using graph neural network

Soumya Sanyal,<sup>1,\*</sup> Arun Kumar Sagotra,<sup>2,†</sup> Narendra Kumar,<sup>3</sup> Sharad Rathi,<sup>4</sup> Mohana Krishna,<sup>4</sup> Nagesh Somayajula,<sup>5</sup> Durairvelan Palanisamy,<sup>6</sup> Ram R. Ratnakar,<sup>7</sup> Suchismita Sanyal,<sup>6</sup> Partha Talukdar,<sup>8,\*</sup> Umesh Waghmare,<sup>3</sup> and Janakiraman Balachandran<sup>2,†</sup>

<sup>1</sup>*University of Southern California, USA*

<sup>2</sup>

<sup>3</sup>*Jawaharlal Nehru Centre for Advanced Scientific Research, Bangalore*

<sup>4</sup>*Vellore Institute of Technology, Vellore*

<sup>5</sup>*Centura, Colorado, USA*

<sup>6</sup>*Shell Technology Centre Bangalore, Bangalore*

<sup>7</sup>*Shell Technology Centre Houston, USA*

<sup>8</sup>*Google Research, Bangalore, India*

The process of design and discovery of new materials can be significantly expedited and simplified if we can learn effectively from available data. Deep learning (DL) approaches have recently received a lot of interest for their ability to speed up the design of novel materials by predicting material properties with precision close to experiments and ab-initio calculations. The application of deep learning to predict materials properties measured by experiments are valuable yet challenging due to the limited amount of experimental data. Most of the existing approaches to predict properties from computational data have also been directed towards specific material properties. In this work, we extend this approach, by proposing Landscape Crystal Graph Convolution Network(LCGCN), an accurate and transferable deep learning framework based on graph convolutional networks. LCGCN directly learns the potential energy surface (PES) from atomic configurations. This approach can enable transferable models that can predict different material properties. We apply this framework to bulk crystals (i.e.  $\text{Al}_2\text{O}_3$ ), and test it by calculating potential energy surfaces at different temperatures and across different phases of crystal.

## I. INTRODUCTION

The development of next generation technologies in energy, chemicals, electronics and transportation industries are closely tied to the development of new materials with the desired properties [1]. For example in case of

energy, the need of the hour is the development of inexpensive and environmentally safe materials that can generate and store electrons with very high density and efficiency while operating at high power. In case of chemicals, there is a critical need to develop new materials with better catalytic performance [2], as well as those which can make chemicals from alternative feedstock such as recycled plastics.

Historically, discovery of materials has been driven by empiricism, through the knowledge and intuition of researchers working on these problems. Over the past few decades, they are being augmented by the insights and knowledge derived from physics based models, in particular, atomistic models and simulations that can predict the various properties of interest for a wide range of materials [3, 4]. However, these physics based models are computationally expensive and as a result, only aid us to explore a small subset of the materials search space. Further, within this approach, there is no formal way to transfer information and knowledge from one system to another, and from one application to another. Data driven models based on statistics and machine learning can help in speeding up the materials discovery process by providing a framework where algorithms can learn from existing data obtained from models and experiments on a subset of materials and predict the properties and functionalities of new materials. In order to facilitate such developments, various research groups from across the world have also provided free public access to the datasets of material structures [5–9] and properties obtained predominantly from atomistic simulations.

These datasets and other datasets obtained from experiments have been used in the recent literature to develop data driven models to predict material properties [10–13]. Most of these models are based on hand crafted descriptors that are suitable only for certain subset of materials and for targeted properties of interest. However, a transferable model needs to operate on raw data to remove these biases introduced through hand crafted descriptors. In case of materials and molecules, such raw input data are the atoms and their position coordinates. This basic materials information can be

\* Work done while at Indian Institute of Science Bangalore

† Corresponding Author and Work done while at Shell Technology Centre Bangalore; [arunsagotra91@gmail.com](mailto:arunsagotra91@gmail.com) and [janakiraman.balachandran@gmail.com](mailto:janakiraman.balachandran@gmail.com)

naturally expressed in the form of graphs. Graph Neural Networks (GNNs) are a class of deep learning models that have been successfully used to model graph-structured data [14–16]. GNNs can learn to effectively represent a molecular/crystal graph from raw data of atom/bond features and use neural networks to perform regression and classification tasks [17–20]. Recently, Xie *et al.* [13] developed crystal graph convolution neural network (CGCNN) that was able to take this basic structural and chemical information of a crystal as graph to perform graph convolutions on these graphs. They were able to obtain excellent results to predict properties of a wide range of crystals, in their ground-state equilibrium structure. Later, Sanyal *et al.* [21] integrated CGCNN with multi-task learning to further improve the prediction accuracy.

## II. OUTLINE OF THE WORK

Although CGCNN has been used to predict equilibrium properties of materials, many thermodynamic, kinetic and transport properties at non-zero temperatures are determined only after incorporating the phononic contributions that distort the crystal and its atomic components from the equilibrium position. These distortion and the resultant phononic contributions depend upon the potential energy surface (PES) associated with it. PES is a highly non-linear complex function of the chemical composition, symmetry and atomic arrangement of the crystals. Even a small change in these parameters can significantly change the PES. The PES is the input to various statistical approaches such as Monte Carlo and molecular dynamics simulations to predict the phononic degrees of freedom and their influence on various material properties.

Conventionally PES are fitted to explicit function forms from ab-initio simulation results. However, over the past few years gaussian process based machine learning has been applied to develop interatomic potentials for various materials ranging from elemental (amorphous carbon, graphene, boron) [22–24] to multi-elemental (methane) [25]. Although very successful, development of Gaussian Approximation Potential (GAP) [26] requires careful design of experiments to simulate small systems whose inputs are needed to fit the interatomic potentials. Further, there are also challenges in transferring the potential to a new system.

These shortcomings can potentially be overcome by GNN based deep learning approach, in which a model learns from the raw materials data. These models can possibly lead to better transferability across different materials composition, crystal symmetry, atomic arrangements and environments. In this work, we provide an initial demonstration of such transferability and propose LANDSCAPE CRYSTAL GRAPH CONVOLUTION NETWORK (LCGCN), an extension of CGCNN architecture, to predict the PES of alumina ( $Al_2O_3$ ), a material

that serves as the base material for various adsorbent and catalytic applications [27–30]. Specifically, we demonstrate the generalizability of this approach by developing LCGCN models that not only accurately predict PES, but are also transferable across scales, environmental conditions (temperature) and different crystallographic polymorphs, trigonal phase (space group  $R\bar{3}c$ ), cubic phase (space group Ia3), Orthorhombic (space groups Pbca and Pna2<sub>1</sub>) of alumina.

## III. METHODOLOGY

### A. Molecular Dynamics

The data required to train, validate and test the CGCNN models were obtained by performing Molecular Dynamics (MD) simulations. We have performed MD simulations under  $(N, V, T)$  conditions with the LAMMPS code [31]. In these simulations the temperature is kept fluctuating around a setpoint value by using Nosé - Hoover thermostats. We employ simulation boxes, typically varying from 30 to 480 atoms, and apply periodic boundary conditions along the three Cartesian directions. Newton’s equations of motion are integrated using the customary Verlet’s algorithm with a time-step length of  $10^{-3}$  ps. The typical duration of a MD run is of 10 ps. We used interatomic potentials of the Second-Moment tight-Binding-QE<sub>q</sub> (SMTB-Q) form [32].

In this work, employing the above MD protocol, we simulate  $Al_2O_3$  systems comprising of different sizes, environmental temperatures and polymorphs. We pick 10,000 configurations of these systems after thermal equilibration. Unless specified otherwise, the 10,000 configurations were divided into a ratio of 6:2:2 for training, validation and testing of the LCGCN model.

### B. Landscape Crystal Graph Convolution Network(LCGCN)

CGCNN [13] is a graph neural network which focuses on building a crystal graph from a given crystal structure and utilizes graph convolution networks (GCNs) to model the crystal graph and predict their properties with accuracy comparable to *ab initio* physics models. We propose LANDSCAPE CRYSTAL GRAPH CONVOLUTION NETWORK (LCGCN), an extension of CGCNN, that can be used to predict the potential energy surface (PES) of crystal structures. Next, we discuss the details of proposed method LCGCN in detail.

A crystal graph  $\mathcal{G}$  is an undirected multigraph defined by nodes representing atoms and edges representing bonds in a crystal. Formally, let  $\mathcal{G}=(\mathcal{A}, \mathcal{E}, \mathcal{V}, \mathcal{U})$  denote a crystal graph. Here  $\mathcal{A}$  represents the set of atoms in the crystal structure,  $\mathcal{E}=\{(i, j)_k: k^{th} \text{ bond between atom } i \text{ and } j\}$ , is the set of undirected edges denoting the bonds and  $|\mathcal{A}|=N$  is

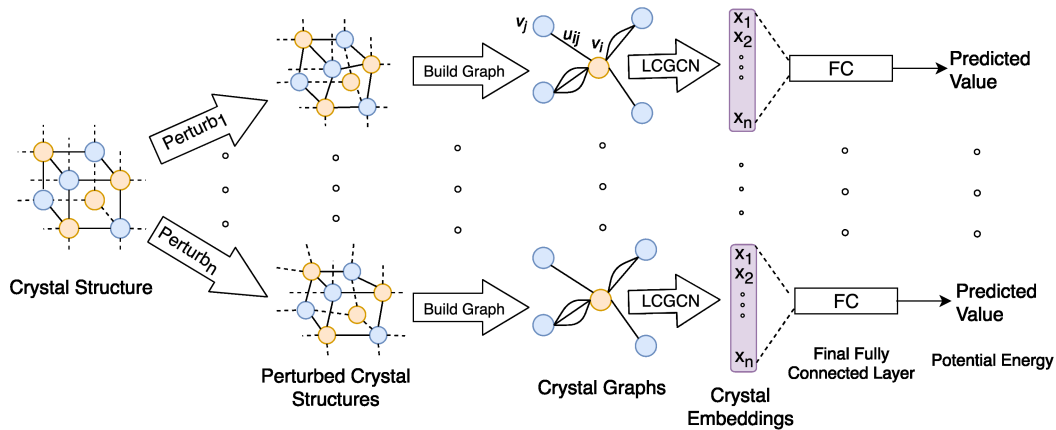


FIG. 1. Schematic representation of using LCGCN to predict potential energy of distorted alumina crystals. Initially, the crystal structure is represented as a graph with nodes and edges representing the atoms and bonds in the crystal respectively. Here,  $\mathbf{v}_i$ ,  $\mathbf{v}_j$  and  $\mathbf{u}_{ij}$  denote the node, neighbor and edge embeddings respectively. Then, CGCNN is used to learn a crystal level embedding  $\mathbf{v}_G$  which is used to predict the potential energy. Please refer to Sec. III B for more details.

the number of atoms in the crystal graph.  $\mathbf{v}_i \in \mathcal{V}$  contains the features of the  $i^{\text{th}}$  atom which encodes various properties of the atom.  $\mathbf{u}_{(i,j)k} \in \mathcal{U}$  is the feature vector for the  $k^{\text{th}}$  bond between atoms  $i$  and  $j$  that captures properties of the edges. To capture the influence of local neighborhood in the crystal structure, a graph convolution formulation similar to CGCNN [13] is used defined as follows,

$$\mathbf{v}_i^{(t+1)} = \mathbf{v}_i^{(t)} + \sum_{j,k} \sigma(\mathbf{z}_{(i,j)k}^{(t)} \mathbf{W}_c^{(t)} + \mathbf{b}_c^{(t)}) \odot g(\mathbf{z}_{(i,j)k}^{(t)} \mathbf{W}_s^{(t)} + \mathbf{b}_s^{(t)}),$$

where  $\mathbf{z}_{(i,j)k}^{(t)} = \mathbf{v}_i^{(t)} \oplus \mathbf{v}_j^{(t)} \oplus \mathbf{u}_{(i,j)k}$  denotes the concatenation of atom and bond feature vectors of the neighbors of  $i^{\text{th}}$  atom.  $\odot$  denotes element-wise multiplication and  $\sigma$  denotes a sigmoid function. The  $\sigma(\cdot)$  factor acts as a learned weight matrix to incorporate different interaction strengths between neighbors.  $\mathbf{W}_c^{(t)}$ ,  $\mathbf{W}_s^{(t)}$ ,  $\mathbf{b}_c^{(t)}$  and  $\mathbf{b}_s^{(t)}$  are the convolution weight matrix, self weight matrix, convolution bias and self bias of the  $t$ -th layer of GCN respectively, and  $g(\cdot)$  is the activation function for introducing non-linear coupling between layers.

Graph pooling [33] is a technique used to learn graph representations given the learnt node and edge features. The learnt atom features are pooled to get a vector representation of the crystal ( $\mathbf{v}_G$ ). The crystal representation  $\mathbf{v}_G$  is then fed to a network of fully-connected layers with non-linearities that learns to predict a property of the crystal in a supervised manner. The workflow is depicted in Fig. 1. To train the network, we calculate the loss using mean squared error between the true values obtained using MD simulations and the model predictions followed by back-propagation [34]. The accuracy of the model is quantified through mean absolute error per atom (MAE/atom) by comparing the model predictions on test configurations against the true values obtained using MD simulations.

Pooling Operator	Formulation
AVERAGE	$\frac{1}{N} \sum_{i=1}^N \mathbf{v}_i$
MAX	$\max(\mathbf{v}_i), \forall i \in [1, N]$
FC-MAX	$\max(\mathbf{v}_i \mathbf{W}_{pool} + \mathbf{b}_{pool}), \forall i \in [1, N]$

TABLE I. Formulation of different graph pooling operators. Here,  $\mathbf{v}_i$  denotes the atom representation and  $\max$  is an elementwise max operator.  $\mathbf{W}_{pool}$  and  $\mathbf{b}_{pool}$  are learnable pooling parameters. Please refer to Sec. IV C for more details.

## IV. RESULTS AND DISCUSSION

### A. Effect of different pooling operators

In this section, we explore some of the existing graph pooling operators - AVERAGE, MAX and FC-MAX. In AVERAGE pooling, the graph embedding is defined as the mean of all the node embeddings. Similarly, for MAX pooling, it is defined as the elementwise max of all the node embeddings. Hamilton *et al.* [33] proposed FC-MAX, a learnable pooling operator, which transforms node embeddings using a fully-connected neural network and then applies MAX pooling operator. The formulation of these pooling operators are defined in Table I. To analyze the effect of pooling, we perform the experiment where we use alumina trigonal polymorph data for training and predict performance on other alumina polymorphs. The results are shown in Table II. We observe that FC-MAX performs the best among all of the pooling operators. And hence, we use FC-MAX as the pooling operator in all further analysis of our LCGCN architecture.

Pooling Operator	Trigonal	Orthorhombic (Pbca)	Orthorhombic (Pna2 <sub>1</sub> )
AVERAGE	0.0009	0.0349	0.1796
MAX	0.0007	0.4256	0.0789
FC-MAX	<b>0.0007</b>	<b>0.0112</b>	<b>0.047</b>

TABLE II. MAE/atom of LCGCN model for different pooling operators on test data of 240 atom alumina orthorhombic (Pbca) and Orthorhombic (Pna2<sub>1</sub>) polymorph trained on trigonal data. Please refer to Sec. IV A for details.

Phase	CGCNN		LCGCN	
	Error/atom	Relative Error	Error/atom	Relative Error
Trigonal	-0.0466	0	-0.0018	0
Orthorhombic (Pbca)	-0.0208	0.0258	0.0001	0.0019
Orthorhombic (Pna2 <sub>1</sub> )	-0.0302	0.0164	0.0031	0.0049

TABLE III. Error/atom (eV/atom) and Relative Error (w.r.t. trigonal alumina phase) of LCGCN and CGCNN model on test dataset of different polymorphs using models trained on setups as defined in Sec. IV B. We observe that LCGCN consistently outperforms CGCNN for all alumina phase equilibrium predictions.

## B. Prediction of energy at equilibrium

Xie *et al.* [13] train their CGCNN model to predict formation energy per atom ( $\Delta E_f$ ) using a large number of equilibrium crystal structures obtained from the Materials Project [5]. Since ( $\Delta E_f$ ) for a large number of crystals can span across a wide range (approximately 8.5 eV/atom), such a model will not be able to accurately predict the small energy differences across different polymorphs of the same composition. However, in this work we train LCGCN model to predict the PES of various polymorphs of alumina through training on distorted input structures obtained from MD simulations. The results are shown in table III. Due to this training data, we expect our model to perform better in predicting the energy differences of the alumina polymorphs. The errors of predictions from the two approaches are shown in table III. We report both 'signed' error and relative error. For relative error, we choose the energy of the trigonal phase as the reference value. As expected, LCGCN significantly outperforms the previous CGCNN model suggesting that LCGCN is well-equipped than CGCNN to predict small energy changes typically seen in distortions. In the next upcoming subsections, we will discuss the PES predictions of alumina across supercell sizes, temperature and polymorphs.

## C. Prediction of potential energy

The LCGCN model was used to predict the potential energy of the trigonal alumina polymorph of different supercell sizes – namely 120 and 480 atoms. The data to train, validate and test was obtained from MD simulations as described in Sec. III A under a temperature ramp of 300K-500K. We quantify the error by reporting mean absolute error per atom (MAE/atom) (eV). The results for the two different supercells are shown in Fig. 2. As expected, increasing the amount of training data reduces the error. We observe that with 0.6 times the total alu-

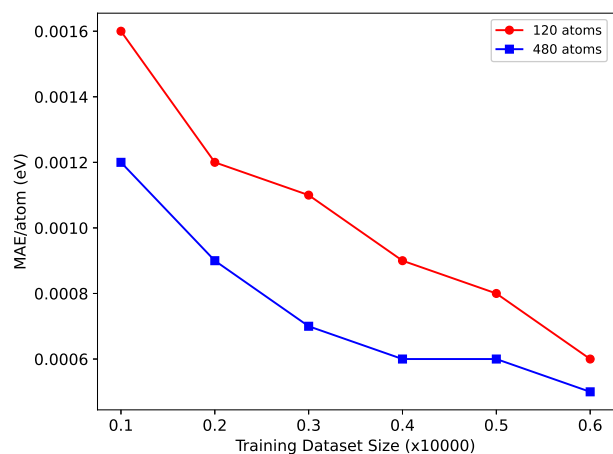


FIG. 2. Plotting test MAE/atom of LCGCN model in predicting potential energy of 120 and 480 atoms systems of alumina trigonal polymorph with increasing size of training dataset. Please refer to Sec. IV C for more details.

mina data (i.e. 6000 samples) for training, our model is able to achieve an MAE/atom which is close to the accuracy of DFT (1 meV/atom).

## D. Transferable LCGCN models across scale

In many scenarios, the property of interest can only be obtained from performing large scale atomistic and quantum mechanical simulations. However, the scaling of such simulations with system size can be non-linear. For example in case of DFT, the cpu time of a simulation increases as  $O(N^3)$  where  $N$  is the number of atoms that limits the system size. Hence, an ML model that is transferable from smaller scale systems to larger scale systems are of importance in the field. Firstly, we note that the cpu time for inference using our model increases as  $O(N)$  with the number of nodes  $N$ . We perform a time analysis of the LCGCN model. For this, we use a

Training		Validation	Testing	MAE/atom
120 atoms	480 atoms	480 atoms	480 atoms	
1000	2400	600	2000	0.0017
3000	2400	600	2000	0.0017
6000	2400	600	2000	0.0011
10000	2400	600	2000	0.0011

TABLE IV. MAE/atom of LCGCN model on test data of 480 atoms with increasing training dataset of 120 atoms. Please refer to Sec. IV D for details.

Training		Validation		Testing	MAE/atom
120 atoms	480 atoms	120 atoms	480 atoms	480 atoms	
2400	0	600	0	2000	0.0023
2400	800	600	200	2000	0.0014
2400	1600	600	400	2000	0.0013
2400	2400	600	600	2000	0.0011

TABLE V. MAE/atom of LCGCN model on test data of 480 atoms with increasing training data of 480 atom configurations. Please refer to Sec. IV D for further details.

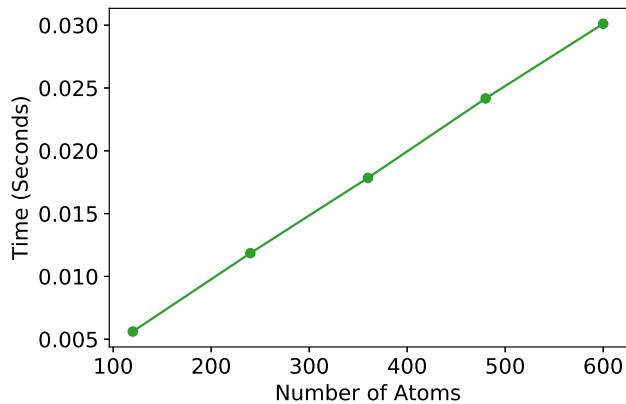


FIG. 3. Time analysis of the LCGCN code with respect to the CPU run, as a function of number of atoms.

pre-trained LCGCN model to predict potential energy for a set of 100 configurations of 120 atom alumina trigonal polymorph. Next, we repeat this for 240, 360, 480 and 600 atoms supercells. The average cpu time for each setup is depicted in Fig. 3. We observe that LCGCN is significantly faster than DFT and MD simulations, and in contrast to MD and DFT the LCGCN scales linearly with the system size and easily parallelized [35, 36].

Next, we demonstrate how increasing the training data of the 120 atoms supercell of alumina trigonal polymorph can reduce the test error of predicting the potential energy of the 480 atom supercell configurations. For this, we consider a setup where there are a fixed 2400 configurations of 480 atoms for model training. Also, we have 10000 configurations of 120 atoms that we progressively add to the training set. As observed from Table IV, an increase in the number of 120 atom configurations in training data leads to a reduction in the test error for the 480 atom configuration. After adding all the 10000 configurations of 120 atoms in training data, the

error in MAE/atom for 480 atom configuration is 0.0011 eV/atom. This is shown in Fig. 4a. In a second set of experiments, the data of 120 atoms is fixed in training set, while the number of 480 atoms is increased in training. The results are reported in Table V and depicted in Fig. 4b. We find that an increase in the 480 atom configuration in training set leads to significant improvements in model performance on predicting potential energy for 480 atoms. From these set of experiments we can conclude that although it is not trivial for LCGCN to generalize, although with comparatively higher error to predict PES of the larger supercell (480 atoms) even when these larger supercell configurations are not included in the training data (1st row of Table V). However, this error goes down significantly even if a small amount of the 480 atoms configurations are included into the training data (4th row of Table V).

### E. Transferable LCGCN models across environmental conditions

Environmental conditions, in particular temperature, play an important role in determining the dynamics of the materials and the resultant phase stability and material properties [1, 37]. Higher temperature molecular dynamics has been employed as a tool in different problems to sample the configurations rapidly and to predict the resultant low energy configuration and their corresponding properties [38]. In this section, we analyze LCGCN’s transferability in predicting potential energies of configurations of trigonal alumina across different environmental conditions. We specifically focus on variation of temperature and test the effectiveness of the model in three temperature values for alumina - 300K, 500K and 800K. We pretrain a LCGCN model using all the data (10,000 configurations) from one temperature and predict potential energy at a different temperature. The results are shown in Table VI.



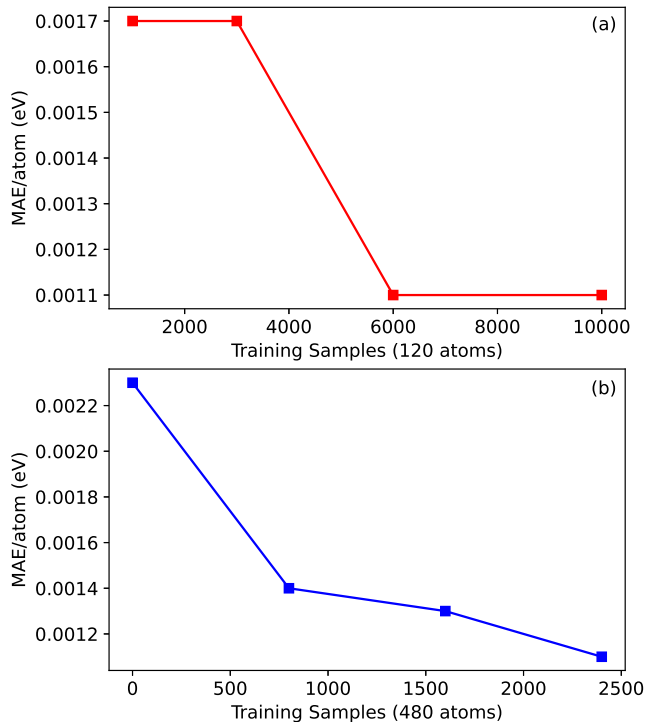


FIG. 4. (a) Test MAE/atom of LCGCN model in predicting potential energy of 480 atoms of alumina trigonal polymorph as a function of increasing training dataset of 120 atoms. Refer Sec. IV D for details. (b) Test MAE/atom of LCGCN model in predicting potential energy of 480 atoms of alumina trigonal polymorph as a function of increasing number of 480 atom configurations in training dataset. Refer to Sec. IV D for details.

In  $\alpha$ - $\text{Al}_2\text{O}_3$ , two types of Al-O bonds (1.87 angstrom and 1.98 angstrom) are present at 0 K. But under classical MD simulation, these two bonds vary drastically at a given temperature  $T$ . At low temperature (say 300 K), bond-bond distribution function shows two peaks (at 1.85 and 2.03 angstrom) while at high temperatures (500 K & 800 K), the peak corresponding to longer (weaker) Al-O bond (2.03 angstrom peak in 300 K configuration) gets disappeared, see Fig. 5a. It means that weakly bonded Al and O got separated much compared to strongly bonded Al and O due to thermal stress.

Next, we observe the effect of mixing the data across two different temperatures (resulting in a total of 20,000 configurations split into training, validation and test set) in predicting energies for data at an unseen temperatures. The results are shown in Table VII. We see when the model is fed with a mixture of two temperatures data for training the prediction error reduces significantly for test data at unseen temperatures. Specifically, we observe a significant decrease in the MAE for prediction at 800K, when data for both 300K and 500K are mixed. In order to delineate if the improvement in model prediction is due to training data volume, or due to data from two different

Temp.	300K	500K	800K
300K	0.0003	0.0212	0.0766
500K	0.0151	0.0004	0.0254
800K	0.0372	0.0192	0.0007

TABLE VI. MAE/atom of LCGCN model on test data of 240 atom alumina trigonal polymorph at three different temperatures. Row temperature indicates that model was trained using the data of that particular temperature and the column temperature denotes that the trained model was used to predict potential energy at that temperature. Please refer to Sec. IV E for more details.

Mixture	Target	MAE/atom
300K & 500K	800K	0.02
300K & 800K	500K	0.0048
500K & 800K	300K	0.0035
300K & 500K(5000 each)	800K	0.0169

TABLE VII. MAE/atom of LCGCN model on test data of 240 atom alumina trigonal polymorph at a target temperature using a mixture of data for two different temperatures in training data. Please refer to Sec. IV E for details.

temperatures, we train a model with 5000 configurations of 300K and 500K each and test the model on data from 800K. The resulting MAE/atom (4<sup>th</sup> row of Table VII) is still significantly lower than predictions at 800K using only 300K or 500K data for training. This suggests that the model is able to learn better when it is trained with heterogeneous data from two different temperatures.

## F. Transferable LCGCN models across different Polymorphs

One of the major challenges in materials and chemistry arises from the difficulty in transferring information, model and knowledge across different crystal structures. A model that can learn properties such as potential energy, from equilibrium and distorted configurations of some crystal structures and predict for new crystal structures with minimal data would be a very useful tool in accelerating materials discovery. As a preliminary step toward this goal, in this work, we study the transferability of LCGCN models across different polymorphs of alumina. We consider three phases of alumina - orthorhombic (Pbca and Pna2<sub>1</sub>) and trigonal. For the first set of experiments, we predict the potential energy of the different polymorphs based on the training data from another polymorph (*aka* zero shot learning). Similar to temperature study, here we use all the data pertaining to a polymorph (10,000 configurations) to train the model. The results are shown in Table VIII.

To understand the trends in the transferability of LCGCN across different polymorphs, we plotted the Al - O bond distribution and configurational energies for the three alumina polymorphs as depicted in Fig. 5b respectively. We observe that, the more the overlap be-

Phase	Orthorhombic (Pbca)	Trigonal	Orthorhombic (Pna2 <sub>1</sub> )
Orthorhombic (Pbca)	0.0007	0.0265	0.037
Trigonal	0.0112	0.0007	0.047
Orthorhombic (Pna2 <sub>1</sub> )	0.9689	0.1542	0.0006

TABLE VIII. MAE/atom of LCGCN model on test data of 240 atom alumina for three different polymorphs. The row phase denotes that the model was trained using the data for that particular polymorph and column phase indicates that the trained model was used to predict the potential energy for that polymorph. Refer to Sec. IV F for more details.

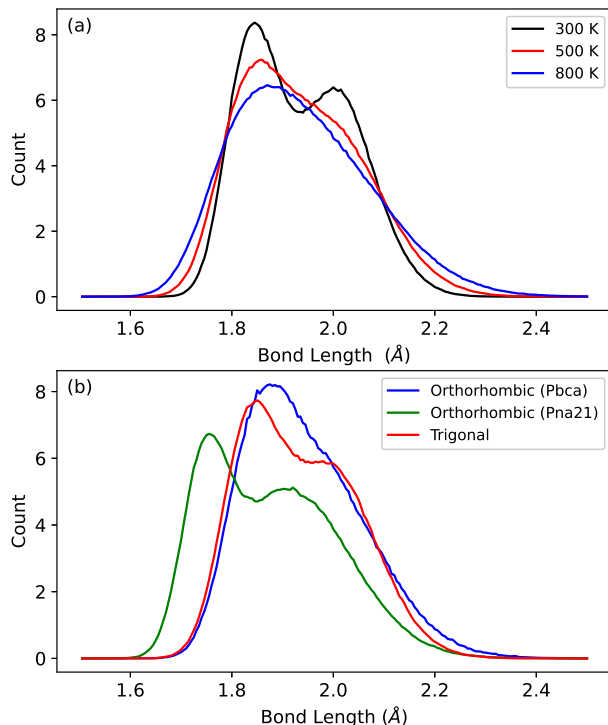


FIG. 5. (a) Al-O bond distribution of  $\alpha$ -Al<sub>2</sub>O<sub>3</sub> at 300 K , 500 K and 800 K temperatures.(b)Al-O bond distribution of Alumina polymorphs. (c) Density of energy distribution of Alumina polymorphs.

Mixture	MAE/atom
Trigonal + Orthorhombic (Pna2 <sub>1</sub> )(5000 each)	0.1804
Trigonal + Orthorhombic (Pna2 <sub>1</sub> )	0.1312

TABLE IX. MAE/atom of LCGCN model on test data of 240 atom alumina orthorhombic (Pbca) polymorph using a mixture of data for different alumina polymorphs in training data. Please refer to Sec. IV F for details.

tween Al – O bond distribution of different polymorphs, the better transferability, and hence lower the error in LCGCN’s prediction. For example, the overlap between the Orthorhombic (Pbca) and Trigonal polymorphs is greater than that between the Orthorhombic (Pbca) and Orthorhombic (Pna2<sub>1</sub>) polymorphs. As seen in Table VIII, our LCGCN model, when trained on Orthorhombic (Pbca) data, predicts the Trigonal polymorph with a lower error compared to when it is trained on Or-

thorhombic (Pna2<sub>1</sub>). This is likely due to the fact that the LCGCN model’s accuracy is highly dependent on bond length, and transferability is better when predicting systems with similar bond lengths.

In order to understand how the model accuracy improves when trained with heterogeneous data, we train the model with data from multiple polymorphs to predict potential energy of orthorhombic (Pbca) polymorph. We choose orthorhombic (Pbca) for our analysis because the error in PES prediction was the highest as shown in Table VIII. The results for this analysis is shown in Table IX. We observe that if we restrict the training data to a total of 10,000 configurations (each polymorph has 5,000 data points), the error in prediction is about 0.1804 eV/atom suggesting that training on diverse dataset can improve the transferability of the model. However, if we incorporate all the data from the two polymorphs (20,000 configurations in total), the model error further reduces to 0.1312 eV/atom suggesting that the transferability of the model can be improved by increasing both the volume and variety of training data.

## V. CONCLUSION

In this work, we proposed LCGCN, a graph neural network framework to directly predict high-dimensional potential energy surface for alumina (Al<sub>2</sub>O<sub>3</sub>), a base material for various adsorbent and catalytic applications, from atomic configurations. This approach enables to bypass calculating the derivatives of the PES which are often the computational bottlenecks of existing *ab-initio* methods.

We further demonstrated the transferability of LCGCN across scales, environmental conditions and different alumina polymorphs. Finally, We validated that, with appropriate conditioning, LCGCN can obtain accuracies that are close to DFT (1 meV/atom). Therefore, we anticipate that LCGCN will significantly accelerate the atomistic studies of other materials with its scalability, versatility, and excellent potential energy surface prediction accuracy.

## DATA AVAILABILITY

The data that support the findings of this study are available from the corresponding author (J.B. and A.K.S) upon reasonable request.

## ACKNOWLEDGMENTS

The authors would like to acknowledge Shell, JNCASR and IISc for their support.

## AUTHOR CONTRIBUTIONS

J.B, U.V.W and P.T conceived the study and planned the research. A.K.S. and N.K. performed the MD simulations to generate the dataset. S.S , M. K, S. R and A.K.S implemented and optimized the LCGCN model. All authors discussed the results and their implications and contributed to the writing of the article.

## COMPETING INTERESTS

The authors declare no competing interests.

- 
- [1] Arun K Sagotra, Dewei Chu, and Claudio Cazorla. Influence of lattice dynamics on lithium-ion conductivity: A first-principles study. *Physical Review Materials*, 3(3):035405, 2019.
- [2] Mohamed Eisa, Dovile Ragauskaitė, Sushil Adhikari, Federico Bella, and Jonas Baltrusaitis. Role and responsibility of sustainable chemistry and engineering in providing safe and sufficient nitrogen fertilizer supply at turbulent times. *ACS Sustainable Chemistry & Engineering*, 10(28):8997–9001, 2022.
- [3] National Science and Technology Council (US). *Materials genome initiative for global competitiveness*. Executive Office of the President, National Science and Technology Council, 2011.
- [4] Narendra Kumar, Padmini Rajagopalan, Praveen Pankajakshan, Arnab Bhattacharyya, Suchismita Sanyal, Janakiraman Balachandran, and Umesh V Waghmare. Machine learning constrained with dimensional analysis and scaling laws: simple, transferable, and interpretable models of materials from small datasets. *Chemistry of Materials*, 31(2):314–321, 2018.
- [5] Anubhav Jain, Shyue Ping Ong, Geoffroy Hautier, Wei Chen, William Davidson Richards, Stephen Dacek, Shreyas Cholia, Dan Gunter, David Skinner, Gerbrand Ceder, and Kristin a. Persson. The Materials Project: A materials genome approach to accelerating materials innovation. *APL Materials*, 1(1):011002, 2013. ISSN 2166532X. doi:10.1063/1.4812323. URL <http://link.aip.org/link/AMPADS/v1/i1/p011002/s1&Agg=doi>
- [6] Stefano Curtarolo, Wahyu Setyawan, Gus LW Hart, Michal Jahnatek, Roman V Chepulskii, Richard H Taylor, Shidong Wang, Junkai Xue, Kesong Yang, Ohad Levy, et al. Aflow: an automatic framework for high-throughput materials discovery. *Computational Materials Science*, 58:218–226, 2012.
- [7] Computational materials database and repositories-nomad. URL <https://nomad-coe.eu/>.
- [8] Arun Mannodi-Kanakkithodi, Gregory M. Treich, Tran Doan Huan, Rui Ma, Matthew Tefferi, Yang Cao, Gregory A. Sotzing, and Rampi Ramprasad. Rational Co-Design of Polymer Dielectrics for Energy Storage. *Adv. Mater. (Weinheim, Ger.)*, 28(30):6277–6291, August 2016. ISSN 0935-9648. doi:10.1002/adma.201600377.
- [9] James E. Saal, Scott Kirklin, Muratahan Aykol, Bryce Meredig, and C. Wolverton. Materials Design and Discovery with High-Throughput Density Functional Theory: The Open Quantum Materials Database (OQMD). *JOM*, 65(11):1501–1509, November 2013. ISSN 1047-4838, 1543-1851. doi:10.1007/s11837-013-0755-4.
- [10] Ghanshyam Pilania, Chenchen Wang, Xun Jiang, Sanguthevar Rajasekaran, and Ramamurthy Ramprasad. Accelerating materials property predictions using machine learning. *Scientific reports*, 3:2810, 2013.
- [11] Logan Ward, Ankit Agrawal, Alok Choudhary, and Christopher Wolverton. A general-purpose machine learning framework for predicting properties of inorganic materials. *npj Computational Materials*, 2:16028, 2016.
- [12] Chiho Kim, Ghanshyam Pilania, and Ramamurthy Ramprasad. From organized high-throughput data to phenomenological theory using machine learning: the example of dielectric breakdown. *Chemistry of Materials*, 28(5):1304–1311, 2016.
- [13] Tian Xie and Jeffrey C. Grossman. Crystal graph convolutional neural networks for an accurate and interpretable prediction of material properties. *Phys. Rev. Lett.*, 120:145301, Apr 2018. doi:10.1103/PhysRevLett.120.145301. URL <https://link.aps.org/doi/10.1103/PhysRevLett.120.145301>.
- [14] Joan Bruna, Wojciech Zaremba, Arthur Szlam, and Yann LeCun. Spectral networks and locally connected networks on graphs. In *International Conference on Learning Representations (ICLR)*, 2014.
- [15] Michael M. Bronstein, Joan Bruna, Yann LeCun, Arthur Szlam, and Pierre Vandergheynst. Geometric deep learning: Going beyond euclidean data. *IEEE Signal Process. Mag.*, 2017.
- [16] Thomas N. Kipf and Max Welling. Semi-supervised classification with graph convolutional networks. In *International Conference on Learning Representations (ICLR)*, 2017.
- [17] David K Duvenaud, Dougal Maclaurin, Jorge Iparraguirre, Rafael Bombarell, Timothy Hirzel, Alan Aspuru-Guzik, and Ryan P Adams. Convolutional networks on graphs for learning molecular fingerprints. In *Advances in Neural Information Processing Systems (NIPS) 28*, pages 2224–2232. Curran Associates, Inc., 2015.



- [18] Steven Kearnes, Kevin McCloskey, Marc Berndl, Vijay Pande, and Patrick Riley. Molecular graph convolutions: moving beyond fingerprints. *Journal of Computer-Aided Molecular Design (CAMD)*, 30(8):595–608, 2016.
- [19] Justin Gilmer, Samuel S. Schoenholz, Patrick F. Riley, Oriol Vinyals, and George E. Dahl. Neural message passing for quantum chemistry. In *Proceedings of the 34th International Conference on Machine Learning (ICML)*, pages 1263–1272, 2017.
- [20] Han Altae-Tran, Bharath Ramsundar, Aneesh S. Pappu, and Vijay Pande. Low data drug discovery with one-shot learning. *ACS Central Science*, 3(4):283–293, 2017.
- [21] Soumya Sanyal, Janakiraman Balachandran, Naganand Yadati, Abhishek Kumar, Padmini Rajagopalan, Suchismita Sanyal, and Partha Talukdar. MT-CGCNN: Integrating crystal graph convolutional neural network with multitask learning for material property prediction. *arXiv preprint arXiv:1811.05660*, 2018.
- [22] Volker L. Deringer and Gábor Csányi. Machine learning based interatomic potential for amorphous carbon. *Phys. Rev. B*, 95:094203, Mar 2017. doi:10.1103/PhysRevB.95.094203. URL <https://link.aps.org/doi/10.1103/PhysRevB.95.094203>.
- [23] Patrick Rowe, Gábor Csányi, Dario Alfè, and Angelos Michaelides. Development of a machine learning potential for graphene. *Phys. Rev. B*, 97:054303, Feb 2018. doi:10.1103/PhysRevB.97.054303. URL <https://link.aps.org/doi/10.1103/PhysRevB.97.054303>.
- [24] Volker L. Deringer, Chris J. Pickard, and Gábor Csányi. Data-driven learning of total and local energies in elemental boron. *Phys. Rev. Lett.*, 120:156001, Apr 2018. doi:10.1103/PhysRevLett.120.156001. URL <https://link.aps.org/doi/10.1103/PhysRevLett.120.156001>.
- [25] Max Veit, Sandeep Kumar Jain, Satyanarayana Bonakala, Indranil Rudra, Detlef Hohl, and Gábor Csányi. Equation of state of fluid methane from first principles with machine learning potentials. *Journal of Chemical Theory and Computation*, 15(4):2574–2586, 2019. doi:10.1021/acs.jctc.8b01242. URL <https://doi.org/10.1021/acs.jctc.8b01242>. PMID: 30794393.
- [26] Albert P. Bartók, Mike C. Payne, Risi Kondor, and Gábor Csányi. Gaussian approximation potentials: The accuracy of quantum mechanics, without the electrons. *Phys. Rev. Lett.*, 104:136403, Apr 2010. doi:10.1103/PhysRevLett.104.136403. URL <https://link.aps.org/doi/10.1103/PhysRevLett.104.136403>.
- [27] József Hlavay and Klára Polyák. Determination of surface properties of iron hydroxide-coated alumina adsorbent prepared for removal of arsenic from drinking water. *Journal of Colloid and Interface Science*, 284(1):71–77, 2005.
- [28] Vinod K Gupta, Shilpi Agarwal, and Tawfik A Saleh. Synthesis and characterization of alumina-coated carbon nanotubes and their application for lead removal. *Journal of hazardous materials*, 185(1):17–23, 2011.
- [29] Herman Pines and Werner O Haag. Alumina: catalyst and support. i. alumina, its intrinsic acidity and catalytic activity1. *Journal of the American Chemical Society*, 82(10):2471–2483, 1960.
- [30] Monica Trueba and Stefano P Trasatti.  $\gamma$ -alumina as a support for catalysts: a review of fundamental aspects. *European journal of inorganic chemistry*, 2005(17):3393–3403, 2005.
- [31] Steve Plimpton. Fast parallel algorithms for short-range molecular dynamics. *Journal of Computational Physics*, 117(1):1 – 19, 1995. ISSN 0021-9991. doi:<https://doi.org/10.1006/jcph.1995.1039>. URL <http://www.sciencedirect.com/science/article/pii/S002199918>.
- [32] N. Salles, O. Politano, E. Amzallag, and R. Tétot. Molecular dynamics study of high-pressure alumina polymorphs with a tight-binding variable-charge model. *Computational Materials Science*, 111:181 – 189, 2016. ISSN 0927-0256. doi:<https://doi.org/10.1016/j.commatsci.2015.09.017>. URL <http://www.sciencedirect.com/science/article/pii/S092702561>.
- [33] William L. Hamilton, Rex Ying, and Jure Leskovec. Inductive representation learning on large graphs. In *NIPS*, 2017.
- [34] David E. Rumelhart, Geoffrey E. Hinton, and Ronald J. Williams. Learning Representations by Back-propagating Errors. *Nature*, 323(6088):533–536, 1986. doi:10.1038/323533a0. URL <http://www.nature.com/articles/323533a0>.
- [35] Justin S Smith, Olexandr Isayev, and Adrian E Roitberg. Ani-1: an extensible neural network potential with dft accuracy at force field computational cost. *Chemical science*, 8(4):3192–3203, 2017.
- [36] Jörg Behler, Roman Martoňák, Davide Donadio, and Michele Parrinello. Pressure-induced phase transitions in silicon studied by neural network-based metadynamics simulations. *physica status solidi (b)*, 245(12):2618–2629, 2008.
- [37] Johan Klarbring and Sergei I Simak. Phase stability of dynamically disordered solids from first principles. *Physical review letters*, 121(22):225702, 2018.
- [38] Jörg Behler and Michele Parrinello. Generalized neural-network representation of high-dimensional potential-energy surfaces. *Physical review letters*, 98(14):146401, 2007.